

# The Membrane Interface as a Structured Compartment and a Substrate for Enzyme Action

OLE G. MOURITSEN, LUIS A. BAGATOLLI, and ADAM C. SIMONSEN

MEMPHYS—Center for Biomembrane Physics, Department of Physics and Chemistry,  
University of Southern Denmark, Odense Denmark

## CONTENTS

1.1	Introduction	3
1.2	Models of Lipid Membranes	5
1.3	Lateral Structure of Lipid Bilayers	6
1.4	Enzymology of Secretory Phospholipase A <sub>2</sub> (s-PLA <sub>2</sub> )	9
1.5	Imaging of s-PLA <sub>2</sub> Action on Lipid Bilayers	11
	Abbreviations	15
	Acknowledgments	15
	References	16

## 1.1 INTRODUCTION

Our picture of the biological membrane has changed considerably over the last few decades mainly due to the advancements in instrumentation that allow us to image membranes with an increasing resolution in space and time. Whereas the picture of the membrane since the introduction of the celebrated Singer–Nicolson fluid-mosaic model [1] has always been one imparting the membrane assembly with considerable dynamics and disorder, the current picture is more refined, describing the membrane as a structured bimolecular and fluid flexible sheet with a certain degree of local lateral organization [2–4] in terms of differentiated lipid domains, in some cases called rafts [5]. Although the lipid-bilayer component

of the membrane is only about 5 nm thick, it is furthermore associated with a distinct transmembrane structure that is described by the so-called lateral pressure profile [6], which displays variations of local stresses corresponding to hundreds of atmospheres across the 5-nm thick bilayer. It is this highly dynamic and still structured and stressful environment that the proteins and enzymes associated with the membranes have to come to terms with in order to carry out their function.

This insight has led to an increasing understanding of the importance of lipids and lipid structure for cell function in general and for protein and enzyme function in particular. By adding to this picture that certain lipids are now also known to act as signaling molecules for a large range of biochemical processes, it becomes clear why lipids and the emerging fields of lipidology and lipidomics have now moved center stage, and the importance of lipids for life sciences is considered to be similar to that of genes and proteins.

This has led to a revival of the study of lipid–protein interactions and of the mutual influence of lipids and proteins on each other. Questions have arisen not only as to how proteins influence the lipid matrix but also as to how the lipids influence protein structure and function. Specific questions cover the insertion and folding of integral membrane proteins, the oligomerization of the protein segments in the plane of the membrane, the structural stability of membrane proteins, the anchoring of proteins in membranes and at membrane surfaces, and the requirement of specific lipids and a certain lipid structure for optimal protein functionality [4, 7].

However, the study of lipids and lipid membranes is complex because of the subtle elements of order that characterize lipid assemblies. Whereas the properties of genes and proteins are described in terms of well-defined molecular structure, the properties of lipids are characterized by terms like variability, diversity, plasticity, adaptability, fluidity, and complexity. The particular role played by lipids is most often determined by their collective properties—that is, properties that cannot be associated with the individual lipid molecule but are consequences of their interactions and cooperative behavior. Examples of such properties are membrane curvature and curvature stress, transbilayer pressure profile, acyl-chain order parameter, packing density, diffusional motion, phase state, and small-scale lateral organization in space and time characterized by a coherence length or equivalently by an average lipid-domain size. Properties like these require quantitative characterization by use of powerful biophysical techniques.

In this present chapter we review some of the results that have been obtained in our laboratories with regard to characterization of lateral order in model bilayer membranes as well as biological membranes, with particular focus on membrane domains in the submicron regime. The results are based mainly on fluorescence microscopy and two-photon laser scanning microscopy as well as atomic force microscopy (AFM). We then show by a specific example how a small enzyme, secretory phospholipase A<sub>2</sub> (s-PLA<sub>2</sub>) becomes activated at membrane interfaces in a way that is controlled by the lateral structure of the lipid-bilayer substrate.

This serves as a clear-cut example of how certain collective properties of a lipid assembly are marshalling the function of a protein, hence highlighting the importance of lipids for membrane function. It furthermore shows how novel instrumentation and imaging techniques open up a new window to allow for quantitative description of biochemical processes.

## 1.2 MODELS OF LIPID MEMBRANES

The generic properties of membranes are conveniently studied by means of well-defined model systems of varying complexity. Here we shall be concerned with rather simple models, specifically unilamellar or multilamellar vesicles (liposomes) as well as solid-supported single bilayers or double bilayers as illustrated in Fig. 1.1. Dispersions of unilamellar or multilamellar vesicles lend themselves to be studied by bulk techniques, such as calorimetry and spectroscopy, whereas individual giant unilamellar vesicles (GUVs, 20  $\mu\text{m}$  mean diameter) conveniently can be investigated by fluorescence microscopy-related techniques [8, 9] or micromechanical techniques. Single- or double-supported bilayers on planar solid surfaces in water are ideally suited to be imaged by fluorescence microscopy or atomic force microscopy techniques. Use of a combination of the various techniques provides a rather complete picture of lipid-bilayer lateral structure, thermodynamics, thermomechanics, and molecular organization. Needless to say, these models can be composed of different types of lipids, for example, one-component systems, mixtures, or natural lipid extracts from cells, possibly reconstituted with proteins or subjected to enzymes that act on the bilayers. Hence the models reflect some properties of real membranes whereas other properties (e.g., asymmetry) are not represented.

Small unilamellar vesicles are formed by extrusion techniques, whereas GUVs are readily formed by electroformation techniques originally developed by Angelova et al. [10]. Multilamellar dispersions are prepared by simple hydration of dry lipids in buffer.

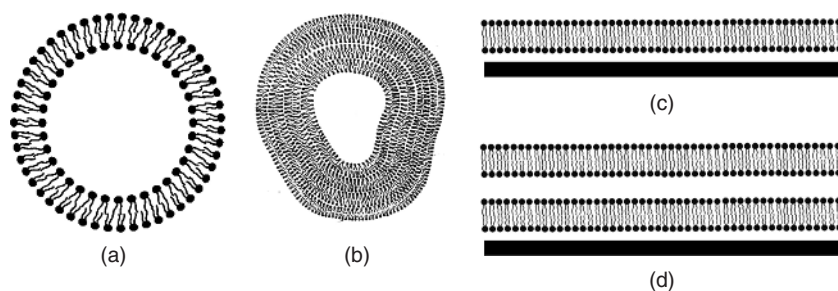


**Figure 1.1** Models of membranes in the form of (a) a unilamellar vesicle (b) a multilamellar vesicle (c) a lipid bilayer on a solid support and (d) a double-supported lipid bilayer.

Single-supported bilayers can be formed by a variety of techniques, including vesicle fusion [11], Langmuir–Blodgett deposition [12] Langmuir–Schaefer deposition [13], self-assembly from solution [14], or hydration of thin, spin-coated lipid films [15]. Double-supported bilayers are more delicate to prepare but can result from vesicle explosion followed by appropriate washing procedures [16]. However, this procedure is not robust for all system compositions and we have found that double-supported membranes can be prepared more reliably by the spin-coating procedure mentioned above. A distinct feature of this method is that dehydrated multiple bilayers are formed during the spin-coating process. The subsequent hydration step merely serves to remove excess bilayers from the surface.

A common substrate surface for supported membranes is muscovite mica, which is hydrophilic and atomically planar, a property that is desirable for AFM measurements. Clean mica surfaces are easily prepared by cleaving the crystal, but it is only semi-transparent and therefore only suitable for high-resolution optical microscopy if the crystal is thin ( $<100\ \mu\text{m}$ ). Glass has ideal optical properties and is suitable as a membrane support if appropriately cleaned. However, most glass is nonplanar with an rms roughness of typically 2–3 nm and this roughness is partially superimposed on AFM measurements and may also interfere with lateral domain formation.

### 1.3 LATERAL STRUCTURE OF LIPID BILAYERS

The distribution of the fluorescent probes in GUVs and planar membranes formed by the same lipid material allows identifying and comparing lipid domains of the same nature and morphology in both systems. Moreover, AFM imaging of the same systems provides additional information on domain formation, which is free of possible interference due to the fluorescent probes. An example of data obtained by these techniques for lipid bilayers composed of POPC and brain ceramide is shown in Fig. 1.2.

Whereas AFM (Fig. 1.2a) furnishes a topological image from which the nature of the domains and phases can only be inferred, and ordinary fluorescence microscopy using probes like DiIc18 fluorescence microscopy (Fig. 1.2b, c) only provides for contrast between different domains, fluorescence microscopy based on for example, LAURDAN generalized polarization (GP) (Fig. 1.2d) allows one to establish structural properties of the coexisting phases, in this case coexisting solid (gel) and fluid domains [17]. Evidence for the solid nature of the domains comes from the LAURDAN emission properties that in turn is reflected in the GP function [9] and is further supported by the observation of the domains being shaped as crystallites with broken domain boundaries.

A more complex case is illustrated in Fig. 1.3 in the case of ternary mixtures of DOPC, DPPC, and cholesterol. In this case cholesterol serves to destabilize solid (gel) phases and introduce liquid-ordered domains whose liquid character is manifested by circular domain interfaces controlled by the line tension of the liquid domains.

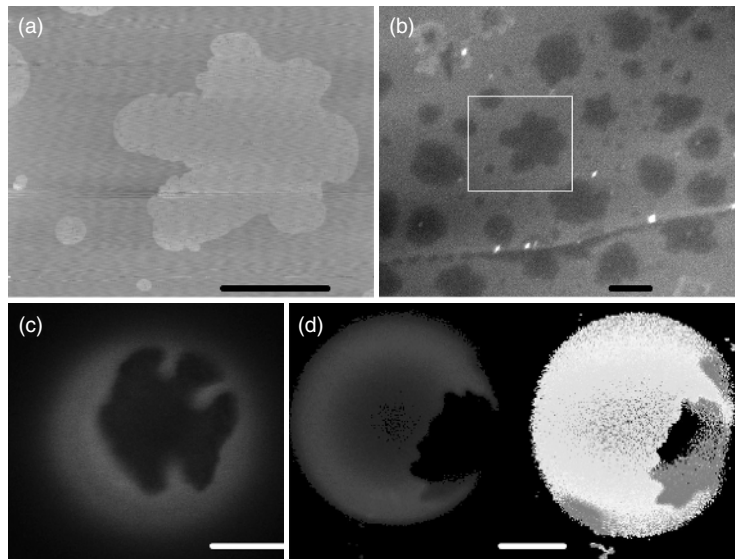


**Figure 1.2** (a) Atomic force microscopy (AFM) image and (b) fluorescence microscopy image of solid-supported bilayers composed of a DiIC18-labeled POPC/brain ceramide 5:1 mol mixture. Giant unilamellar vesicles composed of (c) DiIC18-labeled and (d) LAURDAN-labeled POPC/brain ceramide 5:1 mol mixtures. The scale bars are 5  $\mu\text{m}$ . (Adapted from Ref. 17 where the full color representation can be seen.)

The AFM image in Fig. 1.3a has been obtained on a system of a double-supported bilayer. The round domains are clearly seen in the top bilayer. Domains in the bottom bilayer can barely be seen through the top layer. Such double-supported bilayers can be useful to minimize the effect of the support, which, however, also to some extent can be decoupled from the support by using a 150-mM NaCl solution that tends to screen the electrostatic interaction between the lipid bilayers and the mica support. We have found that double-supported membranes are the class of planar model membranes that most closely mimic the behavior found in GUVs. The dark domains of Fig. 1.3a are in the liquid-ordered state and the bright background phase is in the liquid-disordered state, as established by independent AFM measurements. Fluid domains in such double-supported membranes have round shapes that closely resemble the domains found in GUVs (Fig. 1.3b). The fluid domains are highly mobile and they coalesce upon collision with each other. The domains in the double-supported bilayers and the free bilayers in GUVs resemble to some extent domains found in monolayers on air–water interfaces whose details, however, depend on the lateral pressure applied and the fact that they are bounded by the low-dielectric air space.

Finally, we turn to lipid bilayers with a more complex composition related to real biological membranes. Figure 1.4 shows images of the lateral structure

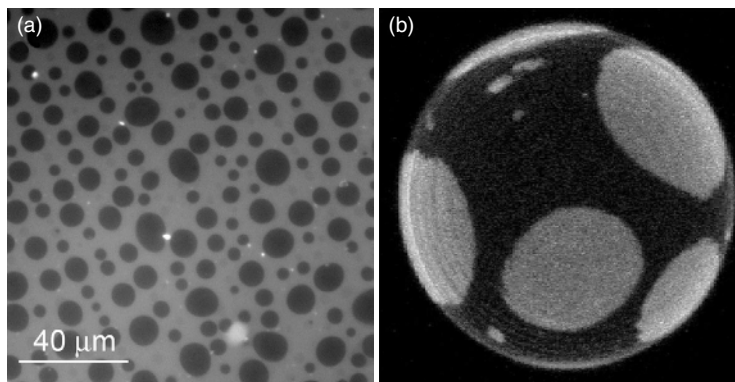


**Figure 1.3** Fluorescence microscopy image of a solid-supported double bilayer formed by hydration of (a) a spin-coated lipid film and (b) a fluorescence microscopy image of a GUV both composed of a DOPC/DPPC/Chol of 2:2:1 mixture at  $T = 20^\circ\text{C}$ . The probes DiIC18 and Bodipy-PC were used in the fluorescent experiments. (Adapted from Refs. 18 and 19.)

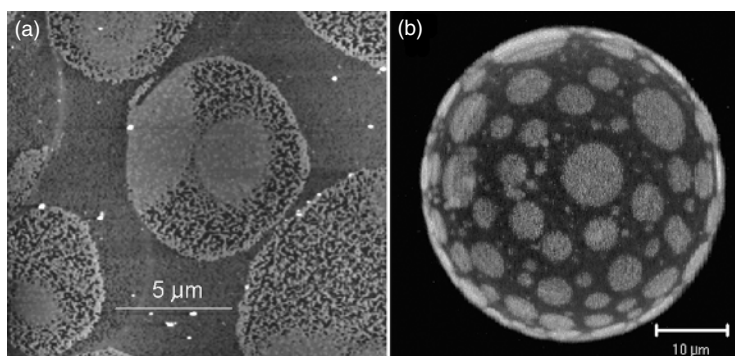


**Figure 1.4** Atomic force microscopy image of (a) a solid-supported bilayer and (b) fluorescence microscopy image of a GUV both composed of native pulmonary surfactant membranes. The circular domains correspond to the liquid-disordered phase, and the fine structure seen in the AFM image (a) is caused by the pulmonary surfactant proteins B and C, which are integral membrane proteins. The probes DiIC18 and Bodipy-PC were used in the fluorescent experiments. (Adapted from Ref. 19.)

of bilayers formed by the natural extract of pig lung surfactants that consist of a complex many-component lipid mixture in addition to integral membrane proteins, the SP-B and SP-C pulmonary surfactant proteins [19]. The major lipid component is DPPC. In addition, the bilayers contain about 20 mol % cholesterol (with respect to phospholipids) whose effect has been shown to introduce a fluid–fluid coexistence pattern with round domains at physiological temperatures.

Additionally, in this particular membranous system, extraction of cholesterol but not extraction of the membrane proteins affects the observed membrane lateral pattern. Specifically, extraction of cholesterol generates a pattern that can be linked with the presence of gel/fluid-like phase coexistence observed in model lipid mixtures. The lateral structure observed in the native pulmonary surfactant at physiological temperatures has been related to the functional properties, for example, the spreading capabilities at air–water interfaces [19]. This observation suggests that pulmonary surfactant could be one of the first membranous systems reported where the coexistence of specialized membrane domains may constitute a structural basis for its function.

#### 1.4 ENZYMOLGY OF SECRETORY PHOSPHOLIPASE A<sub>2</sub> (s-PLA<sub>2</sub>)

s-PLA<sub>2</sub> is a large class of low molecular weight, water-soluble enzymes typically with molar masses below 20 kD. They are found, for example, in venoms, gastric fluids, tear fluid, and inflamed and cancerous tissues. Some act on zwitterionic lipid substrates, whereas others require anionic lipids for being activated. However, they share a common characteristic in that they are interfacially active; that is, they require the lipid substrate to be presented in an organized form, such as a lipid monolayer or bilayer. s-PLA<sub>2</sub> carries out its function by catalyzing the hydrolytic cleavage of the acyl ester bond in the *sn*-2 position, thereby producing lysolipids and a free fatty acid.

The s-PLA<sub>2</sub> from snake venom has a peculiar enzymology that is quite different from Michaelis–Menten kinetics. Rather than being maximally active in the initial state, these enzymes display zero turnover initially and only after a so-called lag time, do they exhibit a rapid burst in activation. This phenomenon is referred to as lag-burst behavior and is illustrated in Fig. 1.5a [20].

Numerous studies have found that the activity of s-PLA<sub>2</sub> is strongly dependent on the structure (or so-called quality) of the lipid substrate and the temperature. In particular, it has been suggested that defects and fluctuations in the layer are nucleation sites for activating the enzyme. Based on rather general considerations, one would expect that there are at least three characteristic contributions to  $\tau$  as illustrated in Fig. 1.5b: (1) a decrease in  $\tau$  upon increasing temperature due to Arrhenius activation of the enzyme; (2) an increase in  $\tau$  upon increasing temperature due to progressive denaturation of the enzyme; and (3) an anomalous minimum at the phase transition of the lipids reflecting the fluctuations in bilayer density in the neighborhood of the lipid-chain melting transition. Depending on the relative positioning and strengths of the three contributions, two possible scenarios for  $\tau(T)$  as shown in Fig. 1.5c arise. Obviously, the location of the phase transition is important for determining whether there are one or two minima in the lag-time behavior.

Figure 1.6 illustrates experimental data for cases with either two minima or a single minimum. A single minimum is found for those lipid bilayers where the phase transition temperature is very low and outside the range of study,

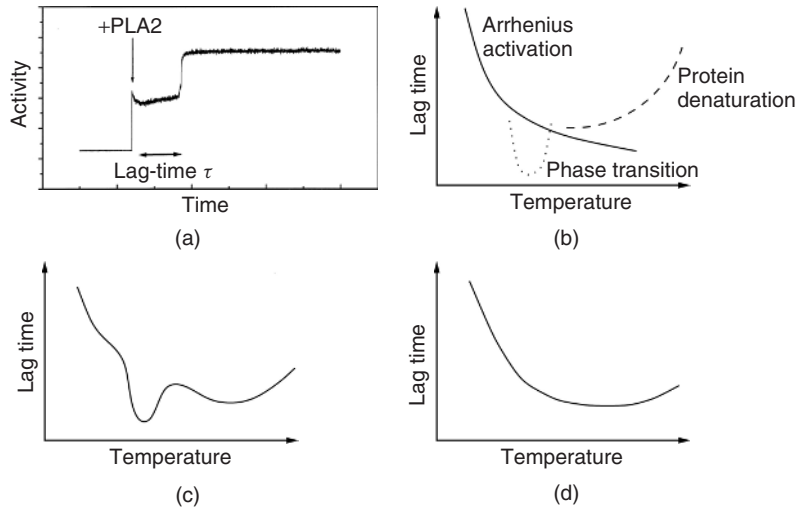


**Figure 1.5** Enzymology of s-PLA<sub>2</sub>. (a) Lag-burst behavior. After a lag period of duration  $\tau$  (the lag time), there is a sudden burst in enzymatic activity here monitored by the intrinsic Trp-fluorescence of the enzyme. (b) There are three contributions to the lag time: Arrhenius activation that tends to enhance the enzyme activity, protein denaturation that diminishes the activity, and an anomalous variation near the phase transition. The three contributions add up to two different scenarios as illustrated in (c) with two local minima and in (d) with a single minimum in the lag time. (Adapted from Ref. 21.)

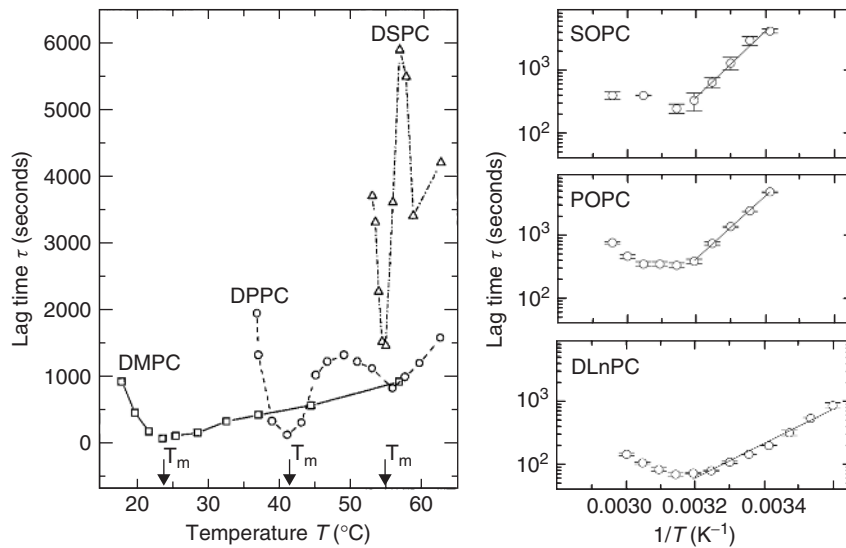


**Figure 1.6** Lag time  $\tau$ , as a function of temperature for the activation of s-PLA<sub>2</sub> for a series of saturated lipids (to the left) and a series of unsaturated lipids (to the right). (Adapted from Refs. 21 and 22.)

for example, e.g. for unsaturated lipids [21]. It is noteworthy that the Arrhenius activated branch for the unsaturated lipid bilayers is associated with an activation energy that correlates with the bending modulus of the bilayers; the softer the bilayer the lower the activation energy.

The anomalous thermal variation of the lag time displayed for the three different saturated lipid bilayers in Fig. 1.6—that is, a short chain lipid (DMPC), an intermediate chain lipid (DPPC), and a long chain lipid (DSPC)—shows that the activity tracks the phase transition with a minimum in  $\tau(T)$  at the respective transition temperature. The minimum is deeper and broader, the shorter the lipid chains. This corroborates the viewpoint that the stronger the lipid-bilayer fluctuations, the more active the enzyme.

The activation characteristics are furthermore very dependent on the type of s-PLA<sub>2</sub>. For example, human s-PLA<sub>2</sub> type IIA does not exhibit a clear lag-burst behavior and furthermore requires anionic lipids for activation [23]. It has been found that there is a lower threshold in terms of minimum charge density on the bilayer surface for activation of the enzyme. This lower threshold, however, can be obtained by local domain formation of the charged lipid species, even in cases where the global charge density is lower than the threshold (e.g., by bringing the bilayer into a phase coexistence region).

## 1.5 IMAGING OF s-PLA<sub>2</sub> ACTION ON LIPID BILAYERS

The effect of the s-PLA<sub>2</sub> on lipid bilayers can readily be investigated by the imaging techniques described earlier on either supported bilayers [24–29] using AFM or fluorescence microscopy, or on GUVs using light [30, 31] or fluorescence microscopy by means of appropriate fluorescence probes [32]. This work supplements the classical work by Ringsdorf and collaborators, who imaged the enzymatic action by fluorescence microscopy in a monolayer assay [33].

In Fig. 1.7 is shown time-resolved fluorescence microscopy images of the lateral structure of a fluid POPC solid-supported lipid bilayer in water subject to s-PLA<sub>2</sub> action. The initially smooth, defect-free bilayer with a few large holes (dark) is subjected to s-PLA<sub>2</sub>, a lag phase follows with very little action, followed by a burst of activity that appears to be nucleated by the preexisting large holes (bottom left), defect lines, and newly formed smaller holes. Eventually, the whole bilayer is digested with some unidentified remains of the products and fluorescent probes at the surface of the support [27].

As shown in Fig. 1.7, the enzyme kinetics of such time-resolved images can be analyzed quantitatively [27, 28] by measuring from the images the areas of the different regions of the bilayer during degradation. The figure shows the total membrane area and its rate of change. Four distinct regimes can be discerned with a clear lag phase and a burst region. After a region of constant activity, there is a linear decrease of area, corresponding to a simple rate equation,  $dA/dt \sim -\sqrt{A}$ ; that is, the area change scales as the perimeter of the domains, which is consistent with the enzyme being activated predominantly at the interfaces that present

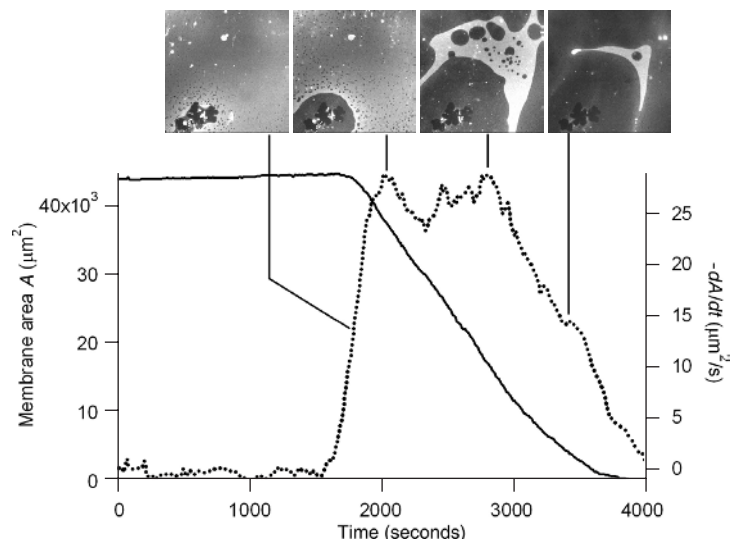


**Figure 1.7** Time evolution of the intact bilayer area (solid line) is shown together with the rate of area change (dotted line) of a fluid POPC lipid bilayer subject to the action of s-PLA<sub>2</sub>. The kinetics is characterized by four distinct regimes: a lag phase, a burst region, a region of constant activity, and a linear region where the area diminishes proportional to the perimeter of the bilayer domains. Typical 120- $\mu\text{m} \times 120\text{-}\mu\text{m}$  images of the lateral structure in the different regions are also shown. (Adapted from Ref. 27.)

themselves as defect lines to the enzyme. Further details of the enzymatic action can be revealed by AFM imaging techniques [24, 25, 34]. Such investigations have also revealed a lag phase and shown that the enzyme is activated at defect lines, such as the rim of holes or at induced defects caused by the accumulation of hydrolysis products.

A particular kind of well-defined nanoscale defect structure is formed in certain lipid bilayers in their so-called ripple phase (cf. Fig. 1.8) that for PC lipids persists over a range of temperatures just below the main phase transition. These ripples can be imaged by atomic force microscopy provided that the bilayer is sufficiently decoupled from the influence of the solid support (e.g., by sitting on top of another bilayer) [26]. In Fig. 1.8 is shown an AFM image of a binary 1:1 DMPC–DSPC bilayer in the ripple phase. The ripples have a periodicity around 26–30 nm and an amplitude around 2–3 nm.

Upon exposure to the enzyme, the ripples are progressively broadened and their amplitude is increased until a critical point, where the bilayer collapses into a flat state. It appears likely that the lipids most prone to attack are those that reside at the top of the ripples.

Turning now to imaging of s-PLA<sub>2</sub> action on GUVs, Figs. 1.9 and 1.10 illustrate the gross morphological changes that the vesicles suffer upon action of the enzyme [32]. Taking advantage of the LAURDAN probe's ability to provide

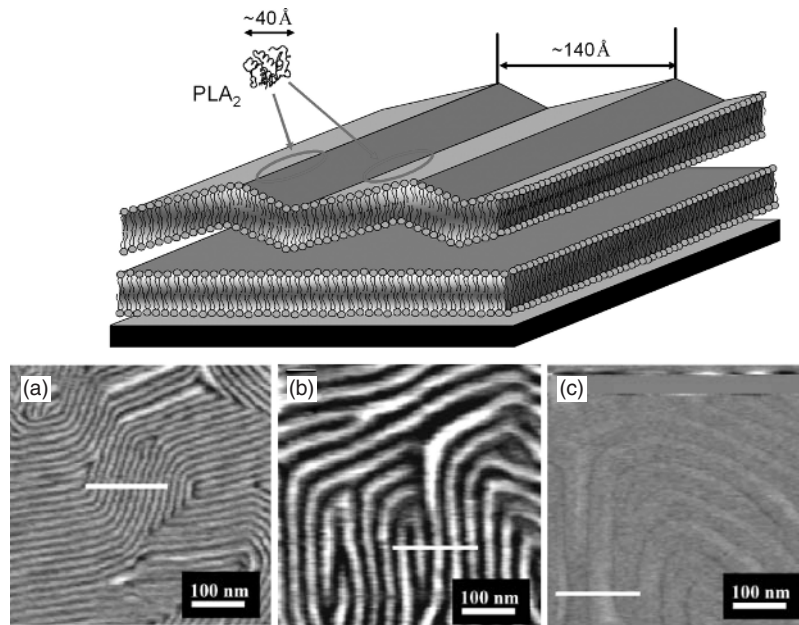


**Figure 1.8** Schematic illustration of a double-supported lipid bilayer exhibiting a rippled structure in the top bilayer, which is only weakly coupled to the support. An approaching s-PLA<sub>2</sub> molecule is shown to scale. Frames (a)–(c) show time-resolved AFM images of the action of s-PLA<sub>2</sub> on solid 1:1 DMPC–DSPC double bilayers at room temperature where the lipids are in the ripple phase. Images are shown for times (a) 0, (b) 77, and (c) 84 min after adding the enzyme. (Adapted from Ref. 26.)

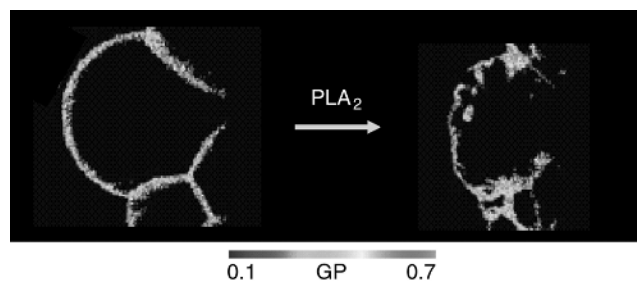


**Figure 1.9** Time-dependent changes in the LAURDAN GP of DMPC GUVs upon addition of s-PLA<sub>2</sub> (*C. Atrox*) at  $T = 26$  °C. The detailed appearance of the GP images in the figure shows formation of small solid domains (orange dot accumulations) suggesting that these regions correspond to product-rich domains formed upon hydrolysis. Presumably, the fatty acid and lysolipid that remain in the bilayer form the basis for these small, high-GP regions. A high GP is indicative of low water penetration that in turn indicates high lipid order or domain formation. (Adapted from Ref. 32 where the correct color representation can be found.)

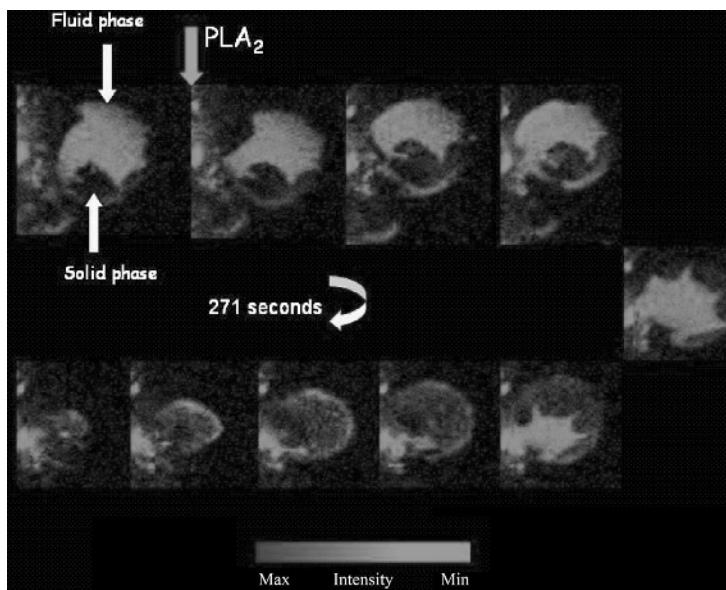


**Figure 1.10** Series of two-photon excitation images of 1:1 DMPE–DMPC GUVs at  $T = 44\text{ }^{\circ}\text{C}$  before and after the addition of a *C. atrox* s-PLA<sub>2</sub>. The fluorescent probe is rhodamine-DPPE. The light and the dark areas in the vesicles correspond to the fluid and gel phases, respectively (grey-scale color representation is according to the scale on the bottom of the figure). (Adapted from Ref. 32.)

information on the structural properties of the lipid domains, the images in Fig. 1.9 indicate that solid domains are formed during the enzymatic action on a single-component GUV. These domains are likely to be enriched in hydrolysis products, in particular, the less water-soluble fatty acids that tend to order the lipid chains.

The effects of s-PLA<sub>2</sub> action on binary lipid mixtures in the form of GUVs are illustrated in Fig. 1.10. At the particular temperature chosen, the bilayer is in a gel/fluid-phase coexistence region and the images show that the fluid phase is more prone to hydrolysis than the solid, gel-phase domains. As observed in the figure the fluid-phase domains are hydrolyzed faster than the solid-phase domains. This observation was made also for GUVs composed of DLPC–DAPC lipid binary mixture. Consistent with these results, a preferential binding of *Crotalus atrox* s-PLA<sub>2</sub> to the fluid-phase domains was also observed in both mixtures.

It is likely that the range of observations of activation of s-PLA<sub>2</sub> described earlier can be rationalized in terms of a common and simple underlying molecular mechanism. It has been proposed [35] that such a mechanism could be protrusion of lipid molecules out of the lipid-bilayer surface as illustrated in Fig. 1.11. Molecular dynamics calculations have shown [21] that such protrusions appear on the time scale of tens of picoseconds with a coherence length of about 0.5 nm.

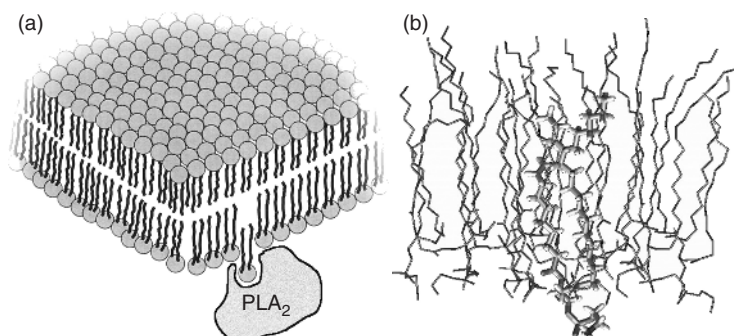


**Figure 1.11** (a) Schematic illustration of an s-PLA<sub>2</sub> molecule bound to a lipid bilayer. The proposed mechanism of a lipid protrusion as a requirement for activating the enzyme to catalyze hydrolysis is shown. (b) A detailed protrusion event of a lipid molecule as observed in a molecular dynamics simulation. (Adapted from Ref. 21.)

Such protrusions would facilitate the entering of a lipid molecule into the active hydrophobic pocket of the enzyme, which is required to initiate hydrolysis. This model is supported by the various findings of phenomena that tend to activate the enzyme: for example, strong fluctuations, softening of lipid bilayers, and defect formation are all expected to enhance protrusion modes.

## ABBREVIATIONS

AFM, atomic force microscopy; Bodipy-PC, 2-(4,4-difluoro-5,7-dimethyl-4-bora-3a,4a-diaza-s-indacene-3-pentanoyl)-1-hexadecanoyl-*sn*-glycero-3-phosphatidylcholine; Chol, cholesterol; DiIC18, 1,1-dioctadecyltetramethyl indotricarbocyanine iodide; DAPC, diarachioyl phosphatidylcholine; DLnPC, dilinoleoyl phosphatidylcholine; DLPC, dilaureoyl phosphatidylcholine; DMPC, dimyristoyl phosphatidylcholine; DMPE, dimyristoyl phosphatidylethanolamine; DOPC, dioleoyl phosphatidylcholine; DPPC, dipalmitoyl phosphatidylcholine; DPPE, dipalmitoyl phosphatidylethanolamine; DSPC, distearoyl phosphatidylcholine; GP, generalized polarization; GUV, giant unilamellar vesicle; LAURDAN: 6-dodecanoil-2-dimethylaminonaphtalene; POPC, 1-palmitoyl,2-oleoyl phosphatidylcholine; SOPC, stearoyl-oleoyl phosphatidylcholine; s-PLA<sub>2</sub>, secretory phospholipase A<sub>2</sub>.

## ACKNOWLEDGMENTS

MEMPHYS-Center for Biomembrane Physics is supported by the Danish National Research Foundation. Chad Leidy has kindly provided us with the illustration of the ripple phase in Fig. 1.8.

## REFERENCES

1. S. Singer and G. L. Nicolson (1972). The fluid mosaic model of cell membranes. *Science* **172**: 720–730.
2. O. G. Mouritsen, (2005). *Life—As a Matter of Fat. The Emerging Science of Lipidomics*. Springer-Verlag, Heidelberg.
3. P. L. Yeagle, (Ed.) (2005). *The Structure of Biological Membranes*, 2nd edition. CRC Press, Boca Raton, FL.
4. L. K. Tamm (Ed.) (2005). *Protein–Lipid Interactions—From Membrane Domains to Cellular Networks*. Wiley-VCH, Weinheim.
5. K. Jacobson, O. G. Mouritsen, and G. W. Anderson (2006). Lipid rafts: at a cross road between cell biology and physics. *Nature Cell Biol.* **9**: 7–14.
6. R. S. Cantor, (1999). Lipid composition and the lateral pressure profile in bilayers. *Biophys. J.* **76**, 2625–2639.
7. M. Ø. Jensen and O. G. Mouritsen (2004). Lipids do influence protein function—the hydrophobic matching hypothesis revisited. *Biochim. Biophys. Acta* **1666**: 205–226.
8. S. L. Veatch and S. L. Keller (2005). Seeing spots: complex phase behavior in simple membranes. *Biochim. Biophys. Acta Mol. Cell Res.* **1746**: 172–185.
9. L. A. Bagatolli (2006). To see or not to see: lateral organization of biological membranes and fluorescence microscopy. *Biochim. Biophys Acta* **1758**: 1541–1556.
10. M. I. Angelova, S. Soleau, P. Meleard, J. F. Faucon, and P. Bothorel (1992). Preparation of giant vesicles by external AC fields. Kinetics and application. *Prog. Colloid Polym. Sci.* **89**: 127–131.
11. A. A. Brian and H. M. McConnell (1984). Allogeneic stimulation of cytotoxic T cells by supported planar membranes. *Proc. Natl. Acad. Sci. USA* **81**: 6159–6163.
12. K. B. Blodgett (1935). Films built by depositing successive monomolecular layers on a solid surface. *J. Am. Chem. Soc.* **57**: 1007–1022.
13. I. Langmuir and V. J. Schaefer (1938). Activities of urease and pepsin monolayers. *J. Am. Chem. Soc.* **60**: 1351–1360.
14. B. A. Cornell, V. L. B. Braach-Maksvytis L. G. King, P. D. O. Osman, B. Raguse L. Wiczorek, and R. J. Pace (1997). A biosensor that uses ion-channel switches. *Nature* **387**: 580–583.
15. A. C. Simonsen and L. A. Bagatolli (2004). Structure of spin-coated lipid films and domain formation in supported membranes formed by hydration. *Langmuir* **20**: 9720–9728.
16. C. Leidy, T. Kaasgaard, J. H. Crowe, O. G. Mouritsen and K. Jørgensen (2002). Ripples and the formation of anisotropic lipid domains: imaging two-component supported double bilayers by atomic force microscopy. *Biophys. J.* **83**: 2625–2663.
17. M. Fidorra, L. Duelund, C. Leidy, A. C. Simonsen, and L. A. Bagatolli (2006). Absence of fluid-ordered/fluid-disordered phase coexistence in ceramide/POPC mixtures containing cholesterol. *Biophys. J.* **90**: 4437–4451.
18. E. J. Morris, M. H. Jensen, and A. C. Simonsen (2006). Domain coarsening in single and double supported ternary membranes with coexisting fluid phases. *Langmuir* **23**: 8135–8141.
19. J. Bernardino de la Serna, J., Perez-Gil, A. C. Simonsen, and L. A. Bagatolli (2004). Cholesterol rules: direct observation of the coexistence of two fluid phases in native

- pulmonary surfactant membranes at physiological temperatures. *J. Biol. Chem.* **279**: 40715–40722.
20. O. G. Mouritsen, T. L. Andresen, A. Halperin, P. L. Hansen, A. F. Jakobsen, U. B. Jensen, M. Ø. Jensen, K. Jørgensen, T. Kaasgaard, C. Leidy, A. C. Simonsen, G. H. Peters, and M. Weiss (2006). Activation of interfacial enzymes at membrane surfaces. *J. Phys. Condens. Matter* **18**: S1293–S1304.
  21. P. Høyrup, T. H. Callisen, M. Ø. Jensen, A. Halperin, and O. G. Mouritsen (2004). Lipid protrusions, membrane softness, and enzymatic activity. *Chem. Phys. Phys. Chem.* **6**: 1608–1615.
  22. T. Hønger, K. Jørgensen, R. L. Biltonen, and O. G. Mouritsen (1996). Systematic relationship between phospholipase A<sub>2</sub> activity and dynamic lipid bilayer microheterogeneity. *Biochemistry* **28**: 9003–9006.
  23. C. Leidy, L. Linderroth, T. L. Andresen, O. G. Mouritsen, K. Jørgensen, and G. H. Peters (2006). Domain-induced activation of human phospholipase A<sub>2</sub> type IIA: local versus global composition. *Biophys. J.* **90**: 3165–3175.
  24. L. K. Nielsen, J. Risbo, T. H. Callisen, and T. Børnholm (1999). Lag-burst kinetics in phospholipase A<sub>2</sub> hydrolysis of DPPC bilayers visualized by atomic force microscopy. *Biochim. Biophys. Acta* **1420**: 266–271.
  25. M. Grandbois, H. Clausen-Schaumann, and H. Gaub (1998). Atomic force microscopy imaging of phospholipid bilayer degradation by phospholipase A<sub>2</sub>. *Biophys. J.* **74**: 2398–2404.
  26. C. Leidy, O. G. Mouritsen, K. Jørgensen, and G. H. Peters (2004). Evolution of a rippled membrane during phospholipase A<sub>2</sub> hydrolysis studied by time-resolved AFM. *Biophys. J.* **87**: 408–418.
  27. U. Bernchou Jensen and A. C. Simonsen (2005). Shape relaxations in a fluid supported membrane during hydrolysis by phospholipase A<sub>2</sub>. *Biochim. Biophys. Acta* **1715**, 1–5.
  28. A. C. Simonsen, U. Bernchou Jensen, and P. L. Hansen (2006). Hydrolysis of fluid supported membrane islands by phospholipase A<sub>2</sub>: time-lapse imaging and kinetic analysis. *J. Colloid Interface Sci.* **301**: 107–115.
  29. P. Moraille and A. Badia (2005). Enzymatic lithography of phospholipid bilayer films by stereoselective hydrolysis. *J. Am. Chem. Soc.* **127**: 6546–6547.
  30. J. Y. Lehtonen P. K. J. Kinnunen (1995). Phospholipase A<sub>2</sub> as a mechanosensor. *Biophys. J.* **68**: 1888–1894.
  31. R. Wick, M. I. Angelova, P. Walde, and P. L. Luisi (1996). Microinjection into giant vesicles and light microscopy investigation of enzyme-mediated transformations. *Chem. Biol.* **3**: 105–111.
  32. S. Sanchez, L. A. Bagatolli, E. Gratton, and T. Hazlett (2002). A two-photon view of an enzyme at work: *C. Atrox* PLA<sub>2</sub> interaction with single-lipid and mixed-lipid giant unilamellar vesicles. *Biophys. J.* **82**: 2232–2243.
  33. D. Grainger, W. A. Reichert, H. Ringsdorf, and C. Salesse (1989). An enzyme caught in action: direct imaging of hydrolytic function of phospholipase A<sub>2</sub> in phosphatidylcholine monolayers. *FEBS Lett.* **252**: 73–82.
  34. T. Kaasgaard, C. Leidy, J. H. Ipsen, O. G. Mouritsen, and K. Jørgensen (2001). *In situ* atomic force microscope imaging of supported bilayers. *Single Mol.* **2**: 105–108.
  35. A. Halperin and O. G. Mouritsen (2005). Role of lipid protrusions in the function of interfacial enzymes. *Eur. J. Biophys. Biophys. Lett.* **34**: 967–971.

